Supporting Information

A Systematic Study of Oxygen Evolution Activity and Stability on $La_{1-x}Sr_xFeO_{3-\delta}$ Perovskite Electrocatalysts in Alkaline Media

Sixuan She[†], Jie Yu[†], Wanqi Tang[†], Yinlong Zhu[†], Yubo Chen[‡], Jaka Sunarso[§], Wei Zhou[*, †] and Zongping Shao[*, †, //]

[†]Jiangsu National Synergetic Innovation Center for Advanced Materials (SICAM), State Key Laboratory of Materials-Oriented Chemical Engineering, College of Chemical Engineering, Nanjing Tech University, No.5 Xin Mofan Road, Nanjing 210009, P.R. China. *E-mail: zhouwei1982@njtech.edu.cn. *E-mail: shaozp@njtech.edu.cn.

[‡]School of Material Science and Engineering, Nanyang Technological University, 50 Nanyang Avenue, Singapore 639798, Singapore.

[§]Faculty of Engineering, Computing and Science, Swinburne University of Technology, Jalan Simpang Tiga, Kuching 93350, Sarawak, Malaysia.

[//]Department of Chemical Engineering, Curtin University, Perth, WA 6845, Australia.
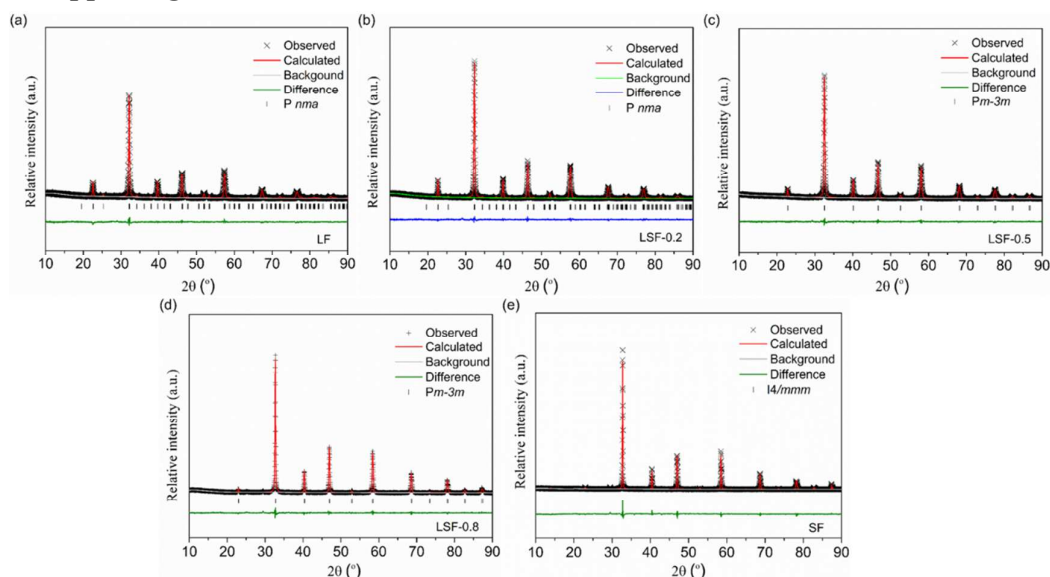
I. Supporting Results

Figure S1 Rietveld refinements plots of the powder X-ray diffraction patterns of the $La_{1-x}Sr_xFeO_{3-\delta}$ (x = 0, 0.2, 0.5, 0.8, and 1) powders, i.e. (a) LF; (b) LSF-0.2; (c) LSF-0.5; (d) LSF-0.8; (e) SF.

Table S1 The oxidation state of Fe and the oxygen non-stoichiometry of the $La_{1-x}Sr_xFeO_{3-\delta}$ (x = 0, 0.2, 0.5, 0.8, and 1) powders from iodometric titrations.

Composition	Oxidation state of Fe	δ
LF	2.98	0.01
LSF-0.2	3.12	0.04
LSF-0.5	3.13	0.18
LSF-0.8	3.10	0.35
SF	3.09	0.46

Table S2 Brunauer-Emmett-Teller specific surface area of the $La_{1-x}Sr_xFeO_{3-\delta}$ (x = 0, 0.2, 0.5, 0.8, and 1) powders.

Samples	a_{s},BET ($m^2\ g^{-1}$)
LF	5.6
LSF-0.2	6.0
LSF-0.5	9.0
LSF-0.8	11.5
SF	2.0

Table S3 The relative amounts of the different Fe species of the $La_{1-x}Sr_xFeO_{3-\delta}$ (x = 0, 0.2, 0.5, 0.8, and 1) powders.

Samples	Fe^{4+} (%)	Fe^{3+} (%)	Fe^{2+} (%)	Average valance
LF	6.51	31.35	62.14	2.44
LSF-0.2	7.93	30.18	61.89	2.46
LSF-0.5	11.23	32.04	56.73	2.54
LSF-0.8	12.52	30.97	56.51	2.56
SF	13.60	32.01	54.39	2.59

Table S4 The relative amounts of the four different surface oxygen species of the $La_{1-x}Sr_xFeO_{3-\delta}$ (x = 0, 0.2, 0.5, 0.8, and 1) powders.

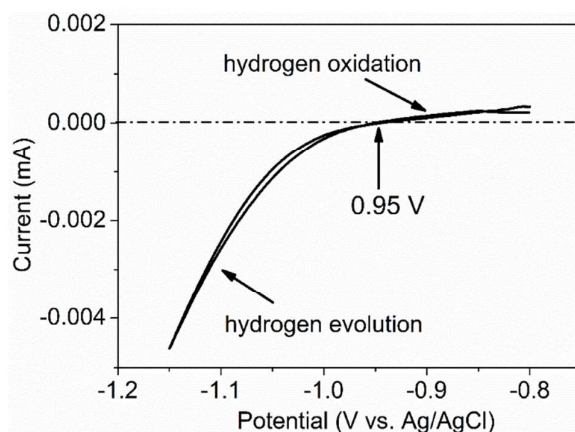| Composition	O^{2-} (%)	O_2^{2-}/O^- (%)	OH^-/O_2 (%)	H_2O (%)
LF	39.09	9.26	44.62	7.03
LSF-0.2	36.07	15.56	39.98	8.40
LSF-0.5	26.79	22.47	36.88	13.86
LSF-0.8	19.59	31.30	41.38	7.73
SF	14.037	24.02	54.52	7.43

Figure S2 Potential calibration of the reference electrode (Ag/AgCl) in 0.1 M KOH solution. The potentials were calibrated by the following equation: $V_{RHE} = V_{Ag/AgCl}+0.95$ V.

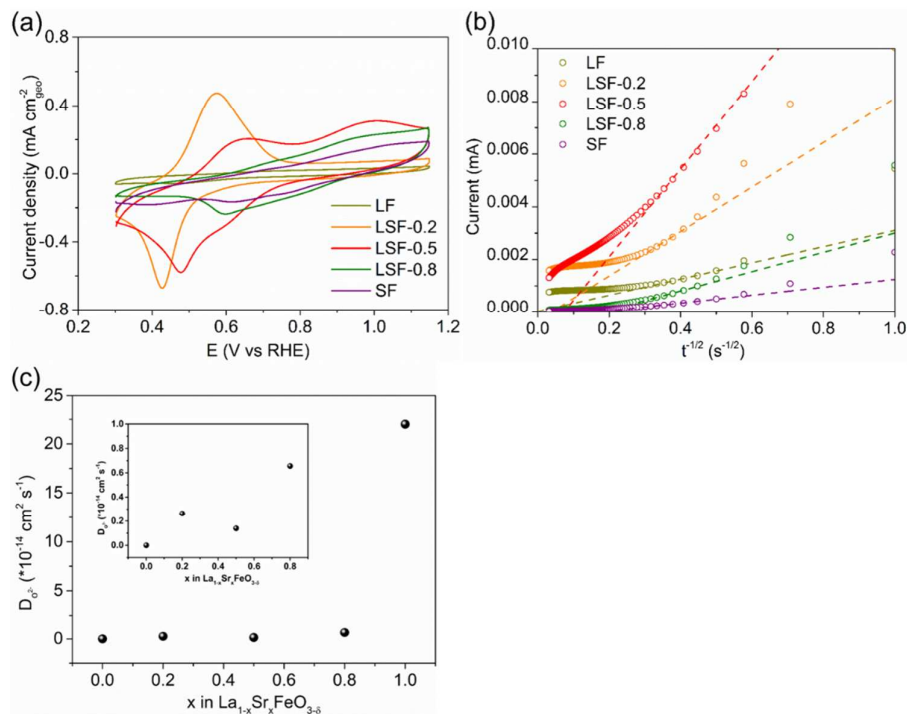**Figure S3** (a) Cyclic voltammetry for the $La_{1-x}Sr_xFeO_{3-\delta}$ (x = 0, 0.2, 0.5, 0.8, and 1) samples obtained at 20 mV s^{-1} scan rate in an Ar-saturated 6 M KOH solution; (b) Current versus t$^{-1/2}$ for the $La_{1-x}Sr_xFeO_{3-\delta}$ (x = 0, 0.2, 0.5, 0.8, and 1) powders; and (c) Oxygen ionic diffusion rate measured from chronoamperometric test at 25 °C. Inset figure displays the oxygen ionic diffusion rate values more clearly for LF, LSF-0.2, LSF-0.5, and LSF-0.8.

The oxygen ions electrochemical insertion and removal (redox) reactions of the 800 °C calcined $La_{1-x}Sr_xFeO_{3-\delta}$ (x = 0, 0.2, 0.5, 0.8, and 1) powders were probed using cyclic voltammetry (CV) in an Ar-saturated 6 M KOH solution; the results of which are shown in **Figure S3a**. The positions of the redox peaks are shifted to higher potentials with an increase in Sr^{2+} content (x) and an increase in oxygen non-stoichiometry (that typically represents the amount of oxygen vacancies) (**Table S1**). Such shift indicates faster oxygen ionic diffusion rate.

The diffusion rate of oxygen ions of LF, LSF-0.2, LSF-0.5, LSF-0.8, and SF were measured by chronoamperometric tests using a bounded 3D solid-state diffusion model with an RDE at 1600 rpm rotation rate in an Ar-saturated 6 M KOH solution.[1] As shown in **Figure S3b**, the intersection of i vs. t$^{-1/2}$ at I = 0 corresponds to $\lambda = a/(Dt)^{1/2}$, where λ is a dimensionless shape factor, a is the radius of the particle, D is the diffusion rate, and t$^{-1/2}$. Given a, and an appropriate shape factor, λ, the diffusion

rate can be measured. In this case, λ was chosen as 2, which is representative of a rounded parallelepiped, halfway between the values for a sphere ($\lambda = 1.77$) and a cube ($\lambda = 2.26$). The value of a is calculated according to the relation of the surface area to particle size for a sphere: $SA = 6/2a\rho$, where ρ is the density of LSF-x. The crystallite sizes (a) of these five samples vary from 9 nm to 55.2 nm due to their different BET surface areas and crystal structures (**Table S4**). As a precaution note, it is more valid to compare diffusion rate for samples with similar crystallite size such as LSF to LSF-0.2 and LSF-0.5 to LSF-0.8. For example, at room temperature, LSF-0.8 that has an oxygen non-stoichiometry (δ) of 0.35 has an oxygen diffusion rate (D) of $4.5 \cdot 10\text{-}15 \text{ cm}^2 \text{ s}^{-1}$, which is higher than that for LSF-0.5 of $1.4 \cdot 10\text{-}15 \text{ cm}^2 \text{ s}^{-1}$ with an oxygen non-stoichiometry (δ) of 0.18 (**Figure S3c**).

References

1. Mefford, J. T.; Rong, X.; Abakumov, A. M.; Hardin, W. G.; Dai, S.; Kolpak, A. M.; Johnston, K. P.; Stevenson, K. J. Water Electrolysis on $La_{1-x}Sr_xCoO_{3-\delta}$ Perovskite Electrocatalysts. *Nat. Commun.* **2016**, 7, 11053.